DE GRUYTER
OPEN

Microstructure and magnetic properties of Nd-Fe-B-(Re, Ti) alloys

Mariusz Hasiak

Abstract. The microstructure and magnetic properties of nanocomposite hard magnetic Nd-Fe-B-(Re, Ti) materials with different Nd and Fe contents are studied. The role of Re and Ti addition in phase composition and volume fraction of the Nd-Fe-B phase is determined. All samples are annealed at the same temperature of 993 K for 10 min. Mössbauer spectroscopy shows that the addition of 4 at.% of Re to the $Nd_8Fe_{78}B_{14}$ alloy leads to creation of an ineligible amount of the magnetically hard $Nd_2Fe_{14}B$ phase. Moreover, the microstructure and magnetic characteristics recorded in a wide range of temperatures for the $Nd_8Fe_{79-x}B_{13}M_x$ ($x = 4$; M = Re or Ti) alloys are also analyzed.

Key words: microstructure • magnetic properties • Nd-Fe-B alloys

M. Hasiak
Department of Mechanics and Materials Science,
Wrocław University of Technology,
25 Smoluchowskiego Str., 50-370 Wrocław, Poland,
Tel.: +48 71 320 3496, Fax: +48 71 321 1235,
E-mail: Mariusz.Hasiak@pwr.edu.pl

Introduction

Nd-Fe-B materials are very attractive because of their good hard magnetic properties, i.e., high energy product, high coercivity and remanence [1]. These materials have been used in many new applications, such as voice coil motors, magnetic resonance imaging devices and others where a high magnetic field is required. The improvement of the mentioned above hard magnetic properties can be achieved by addition of elements such as Ga, Tb, V, Nb, Zr and others to Nd-Fe-B-based alloys [2, 3]. On the other hand, the production process of hard magnetic materials is also very important in creation of a microstructure which affects the magnetic properties. Therefore, several methods of production are used to reduce the costs and time needed for material preparation [4, 5]. One of the most popular production methods of nanocomposite materials, exhibiting good hard magnetic properties, is a rapid solidification of molten materials on a cooled wheel. It has been reported in several articles [6, 7] that a magnetically hard $Nd_2Fe_{14}B$ phase is desirable and plays a dominant role in the improvement of the magnetic properties of obtained materials.

The aim of this paper is to study the effect of Re or Ti addition on microstructure of Nd-Fe-B alloy with different Nd content and its hard magnetic properties.

Experimental procedure

The as-quenched Nd-Fe-B alloys with addition of Re and Ti were prepared in a form of thin ribbons 0.03 mm thick and 2 mm wide. The two groups of compositions were designed for investigation: 1) $Nd_8Fe_{78}B_{14}$, $Nd_8Fe_{74}B_{14}Re_4$ and $Nd_9Fe_{75}B_{14}Re_4$ and 2) $Nd_8Fe_{79}B_{13}$, $Nd_8Fe_{75}B_{13}Ti_4$ and $Nd_8Fe_{75}B_{13}Re_4$. All samples were produced by a rapid quenching method on a single roller with a linear velocity on the surface of 30 m/s in a protective Ar atmosphere. Isothermal heat treatment at the temperature of 993 K for 10 min was chosen according to results of differential scanning calorimetry (DSC) measurements. X-ray diffractometry with CoK_α radiation in fast scan mode and Mössbauer spectroscopy were used to examine the microstructure of annealed samples. Parameters of the phases identified by X-ray diffractometry were used as initial parameters in the Mössbauer spectra fitting procedure. The experimental Mössbauer spectra were recorded at room temperature by a conventional spectrometer in transmission geometry with a ^{57}Co source in a Rh matrix and about 50 mCi activity. The obtained spectra were fitted within a thin absorber approximation with the help of NORMOS package software [8]. Mössbauer spectra were decomposed into elementary subspectra corresponding to different crystallographic sites of Fe atoms. More detailed Mössbauer data analysis, such as volume fraction of each individual phase and relative intensities, was performed for the first group of compositions, for example. The measurements of magnetization versus temperature for the $Nd_8Fe_{79}B_{13}$, $Nd_8Fe_{75}B_{13}Ti_4$ and $Nd_8Fe_{75}B_{13}Re_4$ alloys were performed in the temperature range of 1.9–800 K by a Physical Properties Measurements System Quantum Design. The DC hysteresis loops were recorded in the temperature range of 50–400 K with the step of $\Delta T = 50$ K by a VersaLab System (Quantum Design). The Curie temperatures were determined for the second group of samples using a differential scanning calorimeter (DSC) with a magnetic support.

Results and discussion

The room temperature Mössbauer spectrum with corresponding subspectra (a) together with the hyperfine field distribution (b) obtained for the $Nd_8Fe_{78}B_{14}$ alloy annealed at 993 K for 10 min are shown in Fig. 1. The spectrum consists of broad, overlapped lines characteristic of disordered structural positions of resonant atoms in an amorphous matrix and is decomposed into four components corresponding to crystalline α-Fe, $Nd_{1-\delta}Fe_4B_4$, $Nd_2Fe_{17}B_x$ and the amorphous phase. The same analysis procedure of the spectra of the investigated alloys was applied to the $Nd_8Fe_{74}B_{14}Re_4$ and $Nd_9Fe_{75}B_{14}Re_4$ samples. The fitted hyperfine parameters are listed in Table 1. It is seen that the $Nd_8Fe_{78}B_{14}$ sample is mostly amorphous (63.7%) and only 16.9% of the hard magnetic $Nd_2Fe_{17}B_x$ phase with the high value of the average hyperfine field is observed. Moreover, the soft magnetic α-Fe and paramagnetic $Nd_{1-\delta}Fe_4B_4$ phases are
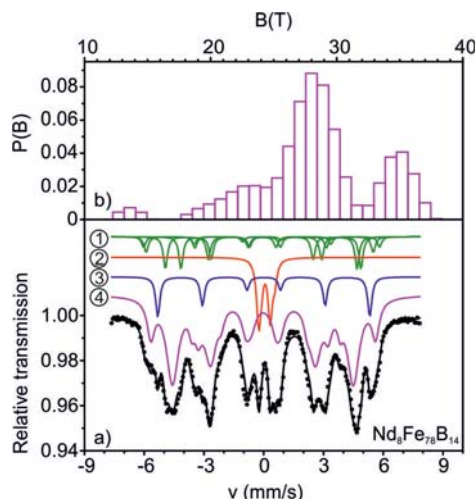
Fig. 1. Transmission room-temperature Mössbauer spectrum together with their spectral components (a) and the corresponding hyperfine field distribution (b) for the $Nd_8Fe_{78}B_{14}$ alloy; (1) − $Nd_2Fe_{17}B_x$, (2) − $Nd_{1-\delta}Fe_4B_4$, (3) − α-Fe and (4) − amorphous phase.

discovered with the volume fractions of 6.1% and 13.3%, respectively. It is worth noting that the hard magnetic $Nd_2Fe_{14}B$ phase is not observed in the $Nd_8Fe_{78}B_{14}$ alloy.

In Fig. 2, the Mössbauer spectrum with corresponding components (a) and hyperfine field distribution (b) for the $Nd_8Fe_{74}B_{14}Re_4$ alloy, where 4 at.% of Fe is replaced by Re atoms, are depicted. One can see that the addition of Re to the $Nd_8Fe_{78}B_{14}$ alloy enables to create of the required $Nd_2Fe_{14}B$ phase, which improves the hard magnetic characteristics, whereas the crystalline $Nd_2Fe_{17}M_x$ phase (M = B or Re) is not detected. The corresponding hyperfine field distribution (Fig. 2b) exhibits a significant high-field peak localized at about 27 T (Table 1). The component with the average hyperfine field of about 24.74 T is ascribed to the amorphous phase with the volume fraction of 41.7%. Moreover, the increase of the volume fraction of the paramagnetic $Nd_{1-\delta}Fe_4B_4$ phase from 13.3% for the Re-free sample to 24.9% in
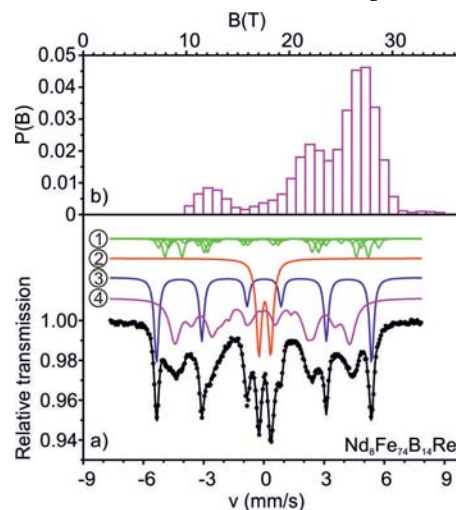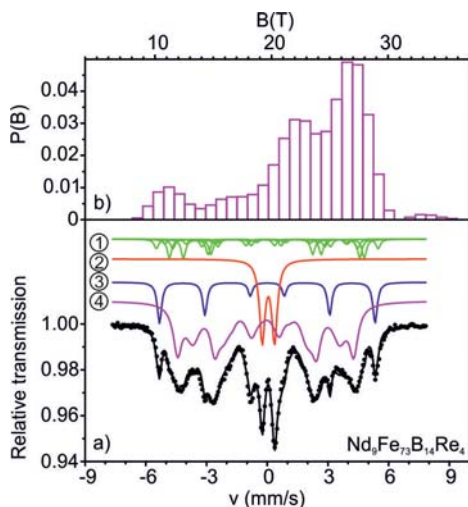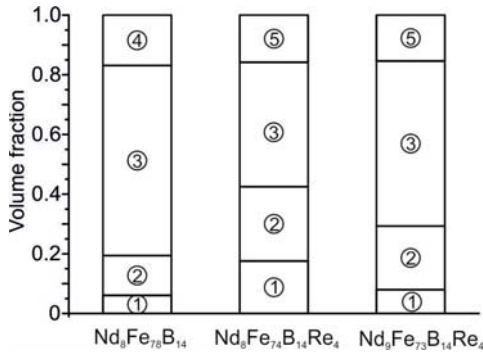

Fig. 2. Transmission room-temperature Mössbauer spectrum together with their spectral components (a) and the corresponding hyperfine field distribution (b) for the $Nd_8Fe_{74}B_{14}Re_4$ alloy; (1) − $Nd_2Fe_{14}B$, (2) − $Nd_{1-\delta}Fe_4B_4$, (3) − α-Fe and (4) − amorphous phase.

Table 1. Mössbauer data obtained from numerical analysis of spectra for the $Nd_8Fe_{78}B_{14}$, $Nd_8Fe_{74}B_{14}Re_4$ and $Nd_9Fe_{75}B_{14}Re_4$ alloys after annealing at 993 K for 10 min. B_{hf} – hyperfine field; IS – isomer shift; QS – quadrupole splitting; Int – relative intensity, and V – volume fraction of phases

Alloy	Phase	Site	B_{hf} [T]	IS [mm/s]	QS [mm/s]	Int [%]	V [%]
	α-Fe		33.00	0	0	7.80	6.1
	$Nd_{1-\delta}Fe_4B_4$			0.033	0.580	7.56	13.3
$Nd_8Fe_{78}B_{14}$	$Nd_2Fe_{17}B_x$	$6c$	36.72	−0.086	−0.045		
		$9d$	35.36	−0.180	−0.048		
		$18h$	30.44	0.018	−0.093	17.56	16.9
		$18f$	27.41	0.094	0.342		
	Amorphous		29.06			67.80	63.7
	α-Fe		33.00	0	0	23.79	17.6
	$Nd_{1-\delta}Fe_4B_4$			0.048	0.583	14.97	24.9
		$4e$	28.01	0.136	−0.450		
		$4c$	24.24	−0.094	0.090		
$Nd_8Fe_{74}B_{14}Re_4$	$Nd_2Fe_{14}B$	$8j_1$	29.77	0.074	−0.043		
		$8j_2$	34.00	0.078	0.319	17.64	15.8
		$16k_1$	28.79	0.141	0.270		
		$16k_2$	29.57	−0.101	−0.115		
	Amorphous		24.74			43.60	41.7
	α-Fe		33.00	0	0	10.98	8.0
	$Nd_{1-\delta}Fe_4B_4$					12.99	21.3
		$4e$	28.00	−0.320	−0.450		
		$4c$	24.52	−0.104	0.090		
$Nd_9Fe_{75}B_{14}Re_4$	$Nd_2Fe_{14}B$	$8j_1$	28.79	0.053	0.053		
		$8j_2$	34.00	−0.022	0.049	17.36	15.4
		$16k_1$	27.71	−0.005	0.270		
		$16k_2$	29.16	−0.093	−0.074		
	Amorphous		23.63			58.67	55.3

the Re-containing sample is derived from the numerical analysis of the Mössbauer spectrum (Table 1).

Figure 3 shows experimental Mössbauer spectrum and its components together with hyperfine field distribution for the sample containing 9 at.% of Nd, i.e., $Nd_9Fe_{73}B_{14}Re_4$ alloy. It is seen that the same phases are created during annealing at 993 K in the $Nd_9Fe_{73}B_{14}Re_4$ alloy as in the previ-

ously discussed $Nd_8Fe_{74}B_{14}Re_4$. The increase one of the Nd content from 8 at.% in the $Nd_8Fe_{74}B_{14}Re_4$ alloy to 9 at.% in the $Nd_9Fe_{73}B_{14}Re_4$ alloy causes only a slight change in the volume fraction of each individual phase, whereas the phase composition remains almost unchanged. It is also worth noting that the hyperfine field distributions for the $Nd_8Fe_{74}B_{14}Re_4$ and $Nd_9Fe_{73}B_{14}Re_4$ alloys demonstrate the same behavior, and magnetically hard magnetic $Nd_2Fe_{14}B$ phase embedded in the amorphous matrix with similar volume fraction is created during the heat treatment.

The changes in the volume fractions of phases in the $Nd_8Fe_{78}B_{14}$, $Nd_8Fe_{74}B_{14}Re_4$ and $Nd_9Fe_{73}B_{14}Re_4$ alloys after annealing at 993 K for 10 min are presented in Fig. 4. It is seen that the amorphous phase occupies more than 40% of the volume fraction of each sample and plays a dominant role in its magnetic properties. The replacement of 4 at.% of Fe atoms by Re ones in the Nd-Fe-B alloy leads to the appearance of the crystalline $Nd_2Fe_{14}B$ phase. It is worth noting that the Mössbauer spectroscopy results are in good agreement with the data of X-ray diffractometry examination.

It is well known that the magnetic properties strictly depend on chemical composition and microstructure. In Figs. 5 and 6, the Mössbauer spectra (a) with corresponding hyperfine field distributions (b) of the $Nd_8Fe_{75}B_{13}Re_4$ and $Nd_8Fe_{75}B_{13}Ti_4$ samples, respectively, are presented. It is well visible that

Fig. 3. Transmission room-temperature Mössbauer spectrum together with their spectral components (a) and the corresponding hyperfine field distribution (b) for the $Nd_9Fe_{73}B_{14}Re_4$ alloy; (1) − $Nd_2Fe_{14}B$, (2) − $Nd_{1-\delta}Fe_4B_4$, (3) − α-Fe and (4) − amorphous phase.

Fig. 4. Volume fractions of individual phases obtained from numerical analysis of the Mössbauer spectra for the $Nd_8Fe_{78}B_{14}$, $Nd_8Fe_{74}B_{14}Re_4$ and $Nd_9Fe_{73}B_{14}Re_4$ alloys; (1) − α-Fe, (2) − $Nd_{1-\delta}Fe_4B_4$, (3) − amorphous phase, (4) − $Nd_2Fe_{17}B_x$ and (5) − $Nd_2Fe_{14}B$.
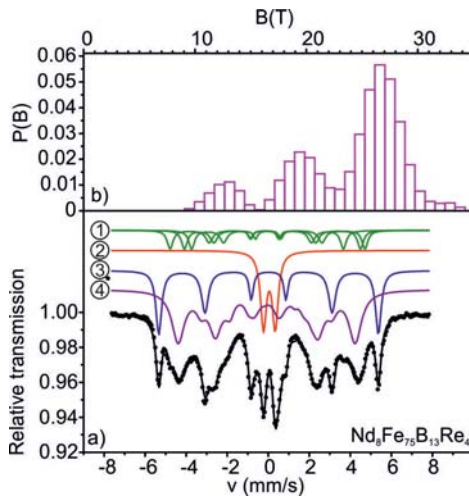

Fig. 5. Transmission room-temperature Mössbauer spectrum together with their spectral components (a) and the corresponding hyperfine field distribution (b) for the $Nd_8Fe_{75}B_{13}Re_4$ alloy; (1) − $(FeNd)_3B$, (2) − $Nd_{1-\delta}Fe_4B_4$, (3) − α-Fe and (4) − amorphous phase.
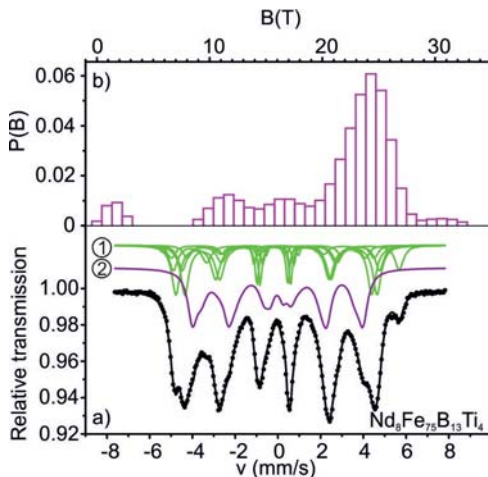

Fig. 6. Transmission room-temperature Mössbauer spectrum together with their spectral components (a) and the corresponding hyperfine field distribution (b) for the $Nd_8Fe_{75}B_{13}Ti_4$ alloy; (1) − $Nd_2Fe_{14}B$ and (2) − amorphous phase.

the partial replacement of Fe atoms by Ti atoms in the master $Nd_8Fe_{79}B_{13}$ alloy, in contrast to the Re--containing sample, leads to formation of substantial amount of the crystalline $Nd_2Fe_{14}B$ phase.
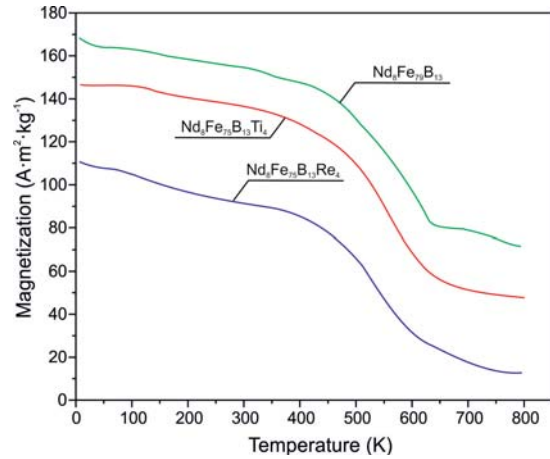
Fig. 7. Temperature dependence of magnetization measured in an external magnetic field of 5 T for the $Nd_8Fe_{79}B_{13}$, $Nd_8Fe_{75}B_{13}Ti_4$ and $Nd_8Fe_{75}B_{13}Re_4$ alloys.

Figure 7 presents the thermomagnetic characteristics, such as magnetization vs. temperature for the $Nd_8Fe_{79}B_{13}$, $Nd_8Fe_{75}B_{13}Ti_4$ and $Nd_8Fe_{75}B_{13}Re_4$ alloys recorded in the temperature range of 1.9–800 K. It is seen that at the external magnetic field of 5 T, the magnetization monotonically decreases, whereas close to the Curie point, a sudden drop of magnetization is observed. The Curie temperatures determined for the investigated alloys are equal to 608 K, 581 and 619 K for the $Nd_8Fe_{79}B_{13}$, $Nd_8Fe_{75}B_{13}Ti_4$ and $Nd_8Fe_{75}B_{13}Re_4$, respectively. Moreover, in the whole investigated temperature range the highest values of magnetization were obtained for the $Nd_8Fe_{79}B_{13}$
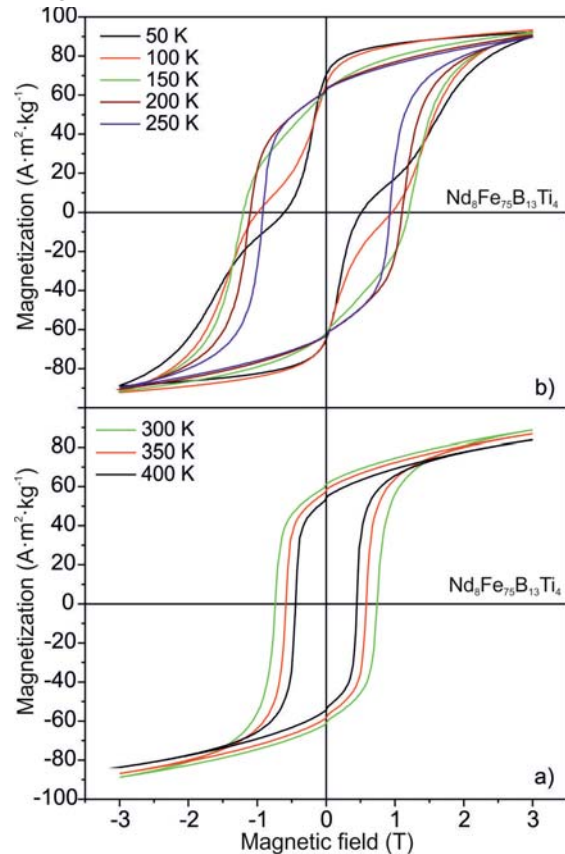
Fig. 8. Exemplary hysteresis loops recorded above (a) and below (b) room temperature for the $Nd_8Fe_{75}B_{13}Ti_4$ alloy annealed at 993 K for 10 min.

alloy, whereas for the Re-containing sample, the magnetization is the lowest (Fig. 7).

The hysteresis loops recorded in the temperature range of 50–400 K for the $Nd_8Fe_{75}B_{13}Ti_4$ alloy are presented, as an example, in Fig. 8. It is seen that the coercivity decreases with the increase of the measurement temperature. Moreover, the magnetic contribution of the discovered phases at temperature below 150 K is clearly visible as the inflection on the shape of the recorded hysteresis loops. The same behavior of the hysteresis loops is observed for the $Nd_8Fe_{79}B_{13}$ and $Nd_8Fe_{75}B_{13}Re_4$ alloys and can be explained as a noncollinear magnetic arrangement below the spin reorientation transition in the $Nd_2Fe_{14}B$ phase [9]. It is also noteworthty that due to the decrease of the coercivity dependence on temperature their application as hard magnetic materials not to be seem possible at temperatures higher than 500 K.

Conclusions

– Mössbauer spectroscopy allows not only reliable identification of the crystalline phases but also the estimation of their relative contributions to the studied alloys.
– The $Nd_8Fe_{78}B_{14}$ alloy annealed at 993 K for 10 min exhibits the presence of the crystalline α-Fe, $Nd_{1-\delta}Fe_4B_4$, $Nd_2Fe_{17}B_x$ and amorphous phases.
– The addition of Re and Ti to Nd-Fe-B alloys leads to the creation of the magnetically hard $Nd_2Fe_{14}B$ phase.
– The shape of hysteresis loops recorded in a wide range of temperature shows that magnetic interactions change with temperature, and structural effects play the dominant role at low temperature.

References

1. Matsuura, Y. (2006). Recent development of Nd-Fe-B sintered magnets and their applications. *J. Magn. Magn. Mater.*, *303*, 344–347. DOI: 10.1016/j.jmmm.2006.01.171.
2. Leonowicz, M. (1990). Magnetic properties and microstructure of $Nd_{16}Fe_{76-x}M_xB_8$ magnets (M = Ga, Cr, Nb, Bi, Sn, Zr, W, V, Mo, Mn). *J. Magn. Magn. Mater.*, *83*, 211–213. DOI: 10.1016/0304-8853(90)90489-D.
3. Chang, H. W., Shih, M. F., Chang, C. W., Hsieh, C. C., Fang, Y. K., Chang, W. C., & Sun, A. C. (2008). Magnetic properties and microstructure of directly quenched $Nd_{9.5}Fe_{75.5-x}M_xB_{15}$ (M = Mo, Nb, Ta, Ti, V, and Zr; x = 0-4) bulk magnets. *J. Appl. Phys., 103*, 07E105–07E105-3. DOI: 10.1063/1.2828516.
4. Olszewski, J., Zbroszczyk, J., Hasiak, M., Kaleta, J., Nabiałek, M., Brągiel, P., Sobczyk, K., Ciurzyńska, W. H., Świerczek, J., & Łukiewska, A. (2009). Microstructure and magnetic properties of Fe-Co-Nd-Y-B alloys obtained by suction casting method. *J. Rare Earths*, *27*, 680–683. DOI: 10.1016/S1002-0721(08)60315-4.
5. Innoue, A. (2000). Stabilization of metallic super-cooled liquid and bulk amorphous alloys. *Acta Mater.*, *48*, 279–306. DOI: 10.1016/S1359-6454(99)00300-6.
6. Manaf, A., Buckley, R. A., & Davies, H. A. (1993). New nanocrystalline high-remanence Nd-Fe-B alloys by rapid solidification. *J. Magn. Magn. Mater.*, *128*, 302–306. DOI: 10.1016/0304-8853(93)90475-H.
7. Durst, K. -D., & Kronmüller, H. (1987). The coercive field of sintered and melt-spun NdFeB magnets. *J. Magn. Magn. Mater.*, *68*, 63–75. DOI: 10.1016/0304-8853(87)90097-7.
8. Brandt, R. A. (1987). Improving the validity of hyperfine field distributions from magnetic alloys: Part I: Unpolarized source. *Nucl. Instrum. Methods Phys. Res. B-Beam Interact. Mater. Atoms*, *28*, 398–416. DOI: 10.1016/0168-583X(87)90182-0.
9. Chaboy, J., García, L. M., Bertolomé, F., Marcelli, A., Cibin, G., Maruyama, H., Pizzini, S., Rogalev, A., Goedkoop, J. B., & Goulon, J. (1998). X-ray magnetic-circular-dichroism probe of a noncollinear magnetic arrangement below the spin reorientation transition in $Nd_2Fe_{14}B$. *Phys. Rev. B*, *57*(14), 8424–8429. DOI: http://dx.doi.org/10.1103/PhysRevB.57.8424.